Determination of load capacity of a non-gasketed flange joint under combined internal pressure, axial and bending loading for safe strength and sealing

Muhammad Abid*[1], Abdul Waheed Awan[1], David H. Nash[2]

[1]Faculty of Mechanical Engineering, GIK Institute of Engineering Sciences and Technology, Topi, NWFP, Pakistan

[2]Department of Mechanical Engineering, University of Strathclyde, Glasgow, UK

ABSTRACT

Performance of a bolted flange joint is characterized mainly due to its 'strength' and 'sealing capability'. A number of analytical and experimental studies have been conducted to study these characteristics only under internal pressure loading. A very limited work is found in literature under combined internal pressure and bending loading. Due to the ignorance of external loads i.e. bending and axial in addition to the internal pressure loading, an optimized performance of the bolted flange joint can not be achieved. The present design codes do not address the effects of combined loading on the structural integrity and sealing ability. To investigate joint strength and sealing capability under combined loading, an extensive comparative experimental and numerical study of a non-gasketed flange joint with two different taper angles on the flange surface and with different load combinations is carried out and overall joint performance and behavior is discussed. Actual joint load capacity is determined under both the design and proof test pressures with maximum additional external loading (axial and bending) that can be applied for safe joint performance.

Keywords: *Non-gasketed, combined, operating, axial, bending, sealing, strength*

*** Corresponding author:** Associate Professor, Faculty of Mechanical Engineering, GIK Institute of Engineering Sciences and Technology, Topi, NWFP, Pakistan, Tel: +92-938-271858, Fax: +92-938-271889, Email: abid@giki.edu.pk

NOTATIONS

υ	*Poisson's ratio*
E	*Young's modulus of elasticity (MPa)*
DP	*Design pressure (15.3 MPa)*
PT	*Proof test pressure (23 MPa)*
FID	*Flange inside diameter (mm)*
FOD	*Flange outside diameter (mm)*
PT	*Pipe top*
PB	*Pipe bottom*
PS	*Pipe side*

For more clarity above mentioned notations are used. Notations used by the design code ASME Appendix-Y for hoop and longitudinal stresses are (S_T *and* S_H) and for flange outside and inside diameters notations are (*A and B).*

1. INTRODUCTION

Different types of flange joints evolved over the centuries and were perfectly adequate for their performance at low pressure and temperature. However, high pressure, temperature and differnt external loading applications led to sealing problems. Leakage (small and large) in flange joints, is a continued significant safety concern in terms of human life, environmental effect and cost. With the rapid advancement in technology for high pressure, high temperature and external loading applications, trends are changing. A flange joint must have adequate mechanical strength and good leak tightness, therefore it is important to evaluate the integrity and sealing performance at actual operating conditions. Available design rules [1,2] for flange joints are mainly concerned with the strength of the flanges and do not sufficiently consider sealing performance. In addition, these do not address the effect of any external loading on the integrity and sealing performance. Non-gasketed flange joints are considered as an alternative due to the 'static mode of load' under

bolt up and different internal pressure [3-8] and temperature loading [9-10], providing better joint strength and sealing capabilities. External loading on bolted flange joints have been discussed in [11-17] but these studies are only for the gasketed flange joints. Similarly other studies [18-20] has been done but these are related to internal pressure plus axial loading but internal pressure plus axial plus bending loading never been properly investigated before.

In this study, a detailed comparative 3D non-linear FEA and experimental study of a non-gasketed flange joint with positive taper angle on flange surface is carried out to investigate its 'Strength' and 'Sealing Capability' under different internal pressures (15.3MPa and 23MPa), axial loadings (180-335kN) and four point bending loadings (68-134kN). The level and distribution of different stress magnitudes and its variation are used to quantify joint strength. Contact or interface pressure variation is used as the main quantitative measure for sealing ability. Non-gasketed flange joint equivalent to four inch 900$^{\#}$ class, with positive taper angle of 0.015 and 0.03 degrees. Both the geometries are analyzed to investigate the most optimum geometry under the applied external loading.

2. ALLOWABLE STRESSES AND FLANGE JOINT CONFIGURATION

Allowable stresses and material properties for flange, pipe, and bolt and symmetry plate are given in Table-1. Material properties for flange is as per ASTM A105 [21], for the bolt and washer is as per ISO898, class 8.8 [22]. Bilinear kinematic hardening for elasto-plastic material properties is used during the analysis. A bilinear material model consists of two sections each having a linear gradient. For the first section, an elastic material is used which is valid until the yield stress and the gradient of this section is the Young's Modulus of Elasticity. The second section functions beyond the yield stress, and gradient (plastic modulus) is 10% [4,23] of the Young's Modulus of Elasticity. The flange dimensions are: thickness = 30mm, taper angle = 0.015degrees (G1) and 0.03degrees (G2), number of bolts = 16 and bolt diameter 10mm. A flange joint equivalent to 4 inch nominal bore of 900# class is used in the study.

3. FINITE ELEMENT MODELLING

In the present work, a complete 360-degree, 3D parametric FE model is used as it eliminates the need for simplifications. Complete 3D model is required to apply the bending loading and constraints at the saddle locations. A combined model of bolt and washer is developed. Stresses in pipe, flange, bolt and contact stress between the flanges under the applied loading are observed. Complete flange and pipe for one side and joint assembly is shown in Fig.1a,b. For FE analysis ANSYS [24] software is used.

3.1. ELEMENT SELECTION AND MESH

Since stresses in flange, bolt, washer and symmetry plate are the required outputs; two classes of elements are used. Solid structural elements (SOLID45) are used for structural stress analysis of the flange joint. Contact elements are used to model contact between different surfaces of the joint. 3D surface-to-surface CONTA173 contact elements, in combination with TARGE170 target elements are used to simulate contact distribution between the flange faces, the top of the flange and the bottom of the washers and bolt shank and bolt holes.

Adaptive meshing is used in the regions of high stress distributions i.e., flange fillet, bolt-hole, bolt head, shank corner, and symmetry plate which are identified on the basis of preliminary studies of the model. Front areas of the model are meshed first and then swept over the volumes for flange, pipe and bolt [Fig. 2].

3.2. BOUNDARY CONDITIONS

Internal pressure is applied at the inside diameter of pipe and flange. Loading due to the head is directly applied as nodal forces across the wall of the pipe. The right flange (where bolts heads rest) is free to move in either axial or radial direction, providing flange rotation to observe exact behaviour of stresses in the flange. Bolts are constrained along centre nodes at the bottom surfaces in x and z-directions and are free to elongate in the y-direction, i.e., axial direction. The second

flange (left flange on bolts ends side) is restricted in axial direction at the nuts location so that it can open during applied loading. Bending load is applied on the areas at a distance of 187mm from the flange centre line. The pipe is supported by the saddles at a distance of 400mm from the flange centre line. Contact is defined between flange ring, bolt head and flange faces. Contact analysis follows a non-linear analysis due to the non-linear behaviour, such as penetration and contact generation. In addition, during the present study, for realistic behaviour of the flange joint components, a non-linear material model is used. All these factors make the problem non-linear. During the solution, the first non-linear solution step is the contact initiation; the second and third non-linear steps use the non-linear material model. During the solution each load step was further divided into number of small sub steps ranging from 10 to 1000. Applied boundary conditions are shown in [Figs.3, 4]. For complete understanding of the applied loading, the following multi-load step procedure is used:

- ***Step 1: Contact initiation:*** Contact between flange top surface and washer bottom is defined by giving a small initial displacement of UY=-0.0052mm in the axial direction to the bolt bottom surface.
- ***Step 2: Pre-stress application:*** A second value of UY=-0.28mm is applied to bolt bottom surface, to achieve initial average pre-stress value of 497MPa in the bolt (which is almost 77%of the yield stress of the bolt material).

  A value of UY=-0.296mm is also applied to achieve initial average pre stress value of 516MPa which is almost 80% of bolt yield stress value.
- ***Step 3: Internal pressure loading***: After pre-stress application, the design pressure and proof test pressure are applied separately for two different cases. End-cap loading as calculated (21.5MPa and 32.3MPa in design and proof test pressures respectively is applied to the end of the pipe, a suitable distance away from the joint [3-9].

- ***Step 4: Combined internal pressure plus axial and bending loading***: The flange joint is analysed under combined internal pressure (design and proof test), axial loading ranging (180~300kN for design pressure and 180~335kN for proof test pressure), i.e., 42~70MPa and 42~78.2MPa in terms of pressure on each side and four point bending loading as lateral load (100~134kN for design pressure plus combined loading and 68~103kN for proof test pressure plus combined loading), i.e., 29.2~39.1MPa and 19.8~30.1MPa in term of pressure on each side to find the exact loading capacity of the joint.

4. EXPERIMENTAL PROGRAM

4.1 FLANGE TYPE, SIZE, TOOLS AND TEST RIG COMPONENTS SELECTION

A non-gasketed flange joint equivalent to four inch, class 900# joint size is selected and an appropriate test rig is fabricated. Reasons for selecting this size are its common use, recommendation of the industrial standards, the ease of handling in the laboratory and the tooling needed. For all tests non-gasketed flange specimens, with and without o-ring, and tools used to make the joint assembly are shown in [Figs. 5a-c]. Flanges and pipe are arranged as per specifications recommended by the codes and industrial standards. End caps at the end of pipe pieces are designed as per PD5500 [25] and remaining calculations for the saddle, frame, pin and side-bars are based on general structural design [4].

4.2 STRAIN GAUGING AND INSTRUMENTATION

To measure strength of test rig comprising of flanges, pipes, bolts and supporting structure, strain gauges are placed on different locations. Connections are made to the data logging system to record results from strain gauges attached at bolts, frame, flange and pipe section. Pressure transducer and test machine are also connected to the data logging system for the measurement of pressure and applied bending loading.

BOLTS: Two strain gauges of 350 Ohm are placed on shank at an angle of 180 degrees on each bolt due to its small diameter and leads are taken out between washer and the bolt head as shown in [Fig. 6a]. Quarter and full bridge circuits are used for strain measurements.

SIDE FRAME: For tests, axial load is applied using a hydraulic pump, and it is measured from a pressure gauge attached to the pump. To measure it accurately digitally during the application of different loading, it is decided to attach two pairs of strain gauges of 120 Ohm on the frame (free end) side plates that hold the pin [Fig. 6b]. The side frame is also calibrated before using it for actual tests. The applied load was calculated from strains recorded.

FLANGE AND PIPE: Four pairs of strain gauges of 120 Ohm resistance are attached at the hub centre and at the hub-flange locations at an angle of 90 degrees. At the hub-flange intersection, strain gauges are attached at the fillet as well as along elliptical portions to note more accurate stress behavior. Four pairs of strain gauges of 120 ohm are attached at an angle of 90 degrees at the pipe centre away from locations of discontinuity [Fig. 6c].

4.3 CALIBRATION OF BOLTS AND RIG AND TEST RIG ASSEMBLY

Calibration plays an important role when undertaking experimental work in order to improve accuracy of the strain measurements. During experiments for combined loading, a combination of equipment is used, e.g., bolts, pressure gauges, pressure transducer, hydraulic pumps, hydraulic pistons, machine for bending load, side frame for axial load and clip gauge for joint opening measurement. To identify interactions between these different components before actual experiments, calibration of different joint components is performed. Using ‘hand-tightening’ methodology with ordinary spanner, sixteen bolts are tightened in sequence 1, 9, 5, 13, 3, 11, 7, 15, 2, 10, 6, 14, 4, 12, 8, and 16 [4].

4.4 TESTING UNDER INTERNAL PRESSURE ONLY

Internal pressure loading is the prime loading as flanged pipe joints are designed to withstand this loading. Pressure loading is applied to the assembled joint via a manually operated hand pump of 50MPa (500 Bar) capacity. Pressure gauges on the pump and pressure transducer on the test vessel are attached to record fluid pressure. Internal pressure loading (up to design pressure of 15.3MPa, proof test pressure of 23MPa and maximum pressure of 40MPa) and unloading was applied in gradual increments and decrements of 0.5MPa (5 Bar) and with sudden pressurization and depressurization and results were recorded. The test rig arrangement is shown in [Fig. 7a].

4.5 TESTING UNDER COMBINED LOADING

In order to observe joint strength and sealing capabilities under combined loading, the following tests were performed.

Test 1: Two sets of tests were performed for this load combination. First, an internal pressure up-to 15.3MPa was applied, and then maintaining this pressure, axial load up-to 180kN was applied. Finally keeping the first two conditions, bending loading as lateral load was applied up-to 134kN. The loads were kept for 10 minutes. During unloading, first bending load then axial and at the end pressure was removed. For the second sequence, first axial load up-to 180kN was applied, and then maintaining this axial load, bending load of 134kN as lateral load was applied. Finally maintaining both these loads, internal pressure up-to 15.3MPa was applied. During unloading, first bending load, then axial, and then pressure at the end was removed. Strains were recorded during all the loading. The joint was continuously monitored for any joint opening at the bottom and the leakage.

Test 2: During this test, during loading, the same sequence was adopted as mentioned in test 1. Whereas during unloading first axial load, then bending and at the end internal pressure applied was removed. Proof test pressure of 23MPa was applied with an axial load up-to 180kN and then

bending to up-to 68kN as lateral load. Strains were recorded during loading and unloading and the joint was monitored for any leakage and opening or gap.

Test 3: This test was performed with the maximum loading conditions. During loading first an axial load of 335kN, followed by a bending load of 103kN was applied. Finally, internal pressure was applied up-to the proof test pressure of 23MPa. Strains were recorded during loading and unloading and the joint was monitored for any leakage and opening or gap. [Fig. 7b].

4.6 EXPERIMENTAL RESULTS DISCUSSION

4.6.1 SEALING

At design pressure: During ***test 1***, at an internal pressure of 15.3MPa and axial load of 180kN, the bending load was increased gradually and the joint was monitored continuously for any possible leak due to joint opening. Opening means relative movement of the two joining flanges in the opposite direction occurring, first along outside diameter, and was measured using feeler gauges. Just above the bending load of 134kN, a gap of 0.05 mm was observed at the bottom. At this load, further application of bending was stopped. This load was kept for 10 minutes, and then the test rig was unloaded as per sequence discussed above. No leakage was observed. During unloading, the joint was monitored and at bending plus axial load, i.e., after removing the pressure, no gap (no bolt relaxation or elongation) was observed.

During ***Test 2***, maintaining an axial load of 180kN and bending load of 134kN, internal pressure was gradually increased and the joint was monitored for any possible leak due to joint opening. At about 15.3MPa, a gap of 0.05 mm was observed at the bottom. This load was kept for 10 minutes, and then the test rig was unloaded as per sequence discussed above and no leak was observed. During unloading, with the applied pressure and axial load, after removing bending, no gap was observed. After unloading of all the loads, no gap, no bolt relaxation or elongation was observed.

At proof test pressure: For this combination, the same methodology was adopted as for Test 2. For both the load sequences, under combined pressure (23MPa), axial load (170kN), and bending load (68kN), no leakage, gap, relaxation and bolt elongation was observed.

4.6.2 STRENGTH

All stresses are calculated from the strains measured along different flange and pipe locations. Two strain gauges are attached at each location i.e. one in hoop and one in axial direction. Hence strains measured are along specified locations.

Hub centre: Maximum axial stress is observed at the top location and is larger than the allowable, and the yield stresses of the flange material. Similarly, hoop stresses at the top location are also larger than allowable stress but less than the yield stress of the flange material. At all other locations, stresses are less than the allowable stress.

Pipe section: At pipe, axial and hoop stresses calculated from the strains are less than the allowable stress of the pipe material for all the applied loading conditions.

Hub-flange fillet: Stresses calculated are within the allowable stress for test 1 and test 2, whereas stresses for the maximum applied loading were larger than the allowable, but were less than the yield stress of the flange material. Due to the small fillet radius, strain gauges of 1.57mm length were also placed to remove any possibility of stress concentration, hence calculated stresses were observed within the allowable limits.

Bolts: For test 1 and test 2, stress results for all the bolts are almost the same and are observed within the allowable limit. Stresses at the inside gauges of bolt 3, 4, 5 and 6 were found larger than the allowable stress, hence the joint opening was observed at the bottom. At the maximum applied loads during test 3, the average stresses calculated for the bolts 3 to bolt 7 in the lower half were close to the yield stress of the bolt. For the bolts in the upper half, the stress difference is small. This shows yielding of the bolts, but the bolts were found in good condition. This shows that the bolts can take higher load than that specified in the code. Bending of the bolts is obvious

for almost all the bolts from the inside and outside gauge readings, which is due to the eccentric and bending loading in the joint.

4.7 STRESS CALCULATIONS FROM EXPERIMENTALLY MEASURED STRAINS

Two strain gauges were attached at each location, i.e., in axial and hoop directions. Stresses calculated from experimentally measured strains at various strain-gauge locations were converted to principle stresses, both in the axial and hoop directions, using the expressions given in equations 1 and 2. FEA stresses are compared with the experimental stress results, at strain gauge locations.

$$\sigma_1 = \frac{E}{1-\nu^2}\left(\varepsilon_1 + \nu\varepsilon_2\right) \quad \ldots\ldots\ldots\ldots(1)$$

$$\sigma_2 = \frac{E}{1-\nu^2}\left(\varepsilon_2 + \nu\varepsilon_1\right) \quad \ldots\ldots\ldots\ldots(2)$$

5 FEA RESULTS DISCUSSION

5.1 STRESS VARIATION IN PIPE

Stress intensity, axial and hoop stresses are found within the allowable stress at;

- Design pressure plus axial load up to 180kN, plus bending load up to 134kN
- Design pressure plus axial load of 300kN, plus bending load up to 100kN.
- Design pressure plus axial load of 335kN, plus bending load up to 103kN.
- Proof test pressure plus axial load up to 180kN and bending load up to 68kN

FEA results are also found in good agreement with the experimental results by Abid [4] and are plotted in [Fig.8].

5.2 STRESS VARIATION IN FLANGE

Stress variation results along flange hub center and flange hub fillet are plotted in Figs. 9-12 and are discussed below;

5.2.1 MAXIMUM STRESS INTENSITY AT HUB FLANGE FILLET

- At design pressure, maximum stress intensity of 215MPa is increased to 229MPa for flange geometry G1, and to 243MPa for flange geometry G2, at an additional axial and bending load of 180kN and 68kN, respectively, at bottom location.
- At proof test pressure, maximum stress intensity of 231MPa is increased to 243MPa for flange geometry G1, and to 255MPa for flange geometry G2, at an additional axial and bending load of 180kN and 68kN, respectively, at bottom location.
- Stress intensity is further increased to 277MPa and 299MPa at design and proof test pressure respectively, at an additional axial and bending load of 335kN and 103kN, respectively, at bottom location.
- Stress intensity observed is larger than the allowable stress limit at design pressure plus axial load of 300kN and proof test pressure plus axial load of 220kN, with any applied additional bending load.

5.2.2 MAXIMUM AXIAL AND HOOP STRESS AT HUB CENTER

- At design pressure, maximum axial stress of 196MPa is increased to 215MPa for flange geometry G1, and to 226MPa for flange geometry G2, at an additional axial and bending load 180kN and 68kN, respectively.
- At proof test pressure, maximum axial stress of 216MPa is increased to 230MPa for flange geometry G1, and to 240MPa for flange geometry G2, at an additional axial and bending load of 180kN and 68kN, respectively.
- Axial stress is further increased to 265MPa and 307MPa at design and proof test pressure, respectively, at an additional axial and bending load of 300kN and 100kN, respectively.
- Maximum axial stress reaches allowable stress limit, at design pressure plus axial load of 300kN and proof test pressure plus axial load of 230kN, with any additional applied bending load.

- At design pressure, maximum hoop stress of 135MPa is increased to 142MPa for flange geometry G1, and to 150MPa for flange geometry G2, at an additional axial and bending load of 180kN and 68kN, respectively.
- At proof test pressure, maximum hoop stress of 159MPa is increased to 164MPa for flange geometry G1, and to 172MPa for flange geometry G2, at an additional axial and bending load of 180kN and 68kN, respectively.
- Hoop stress is further increased to 162MPa and 198MPa at design and proof test pressure respectively, at an additional axial and bending load of 335kN and 103kN, respectively.
- Overall, maximum axial stress observed is with in the allowable stress limit.

5.2.3 MAXIMUM PRINCIPAL STRESS AT HUB CENTER

- At design pressure, maximum principal stress of 244MPa is increased to 261MPa for flange geometry G1, and to 276MPa for flange geometry G2, at an additional axial and bending load of 180kN and 68kN, respectively.
- At proof test pressure, maximum principal stress of 262MPa is increased to 276MPa for flange geometry G1, and to 290MPa for flange geometry G2, at an additional axial and bending load of 180kN and 68kN, respectively.
- Principal stress is further increased to 316MPa and 335MPa at design and proof test pressure respectively, at an additional axial and bending load of 300kN and 100kN, respectively.
- Principal stresses observed are more than the allowable limit but within the yield limit of the flange material under all applied loading.

Overall, comparing FEA stress results with the experimental stress results of Abid [4] at hub centre and hub flange fillet, a slight variation is found due to the possible larger strain gauge and variation during strain measurements.

5.3 STRESS (STRESS INTENSITY AND BENDING STRESS) VARIATION IN BOLTS

FEA and experimental results for maximum stress intensity and axial stress results are plotted in Figures 13-14 under combined loading and are discussed below.

- At design pressure plus axial load of 180kN, maximum stress intensity and axial stress of 590MPa, is increased to 649MPa and 651MPa, respectively, at an additional bending load of 188kN, at the inside diameter of the bolt, at top location for both the flange geometries.
- At proof test plus axial loading of 180kN, maximum stress intensity and axial stress of 594MPa, is increased to 654MPa, at an additional axial and bending load of 335kN and 103kN, respectively.
- At design pressure, maximum stress intensity and axial stress, exceeds the allowable stress limit of the bolt material, at an additional axial and bending load of 180kN and 100kN, respectively.
- At proof test pressure, maximum stress intensity and axial stress, exceeds the allowable stress limit of the bolt material, at an additional axial and bending load of 180kN and 60kN, respectively.
- At design pressure, maximum bolt bending stress of 651~401MPa and 650~435MPa is observed at the inside and outside gauges of the bolts, respectively, at an additional axial and bending load of 180kN and 134kN, respectively for flange geometry G1 and axial and bending load of 300kN and 100kN, respectively, for the flange geometry G2.
- At proof test pressure, maximum bolt bending stress of 644~459MPa is observed at the inside and outside gauges of the bolts, respectively, at an additional axial and bending load of 180kN and 68kN for geometry G2, and 654~434MPa at an additional axial and bending load of 335kN and 103kN for flange geometry G1.

FEA results are compared with the experimental results of Abid. FEA results are different from experimental results because in the case of FEA all the bolts are preloaded to the same stress

level, whereas experimentally, bolts in the joints are tightened one by one, as per specified sequence. However, stress variation trend in each bolt observed is the same.

5.4 CONTACT STRESS BETWEEN FLANGE FACES

Contact stress variation results are plotted in Fig. 15. Results for contact stress variations from inside to outside diameter are plotted in Fig. 16a-b. Results are discussed in detail as follows;

- At design pressure, contact stress of -22MPa is decreased to -3MPa for G1, and to -5MPa for G2, at the bottom location, at an additional axial and bending load of 180kN and 134kN, respectively.
- At proof test pressure, contact stress of -16MPa is decreased to 4MPa for G1 and to -1MPa for G2, at the bottom location, at an additional axial and bending load of 180kN and 68kN.
- A good contact is observed along bolthole lines at the top and bottom locations. This shows the sealing of the joint, at an additional axial and bending load of 335kN and 103kN, respectively, in addition to the design and proof test pressure.

5.5 AXIAL FLANGE DISPLACEMENT

Axial flange displacement results are plotted in Fig. 17 and Figs. 18a-b and are discussed below.

- At the inside diameter of the flange, axial flange displacement of -0.0237mm, at combined design pressure and axial load of 180kN, decreased to -0.0191mm, at an additional bending load of134kN for G1 and -0.0265mm for G2.
- Axial displacement of -0.0191mm, at combined proof test pressure and axial load of 180kN, decreased to -0.0161mm, at an additional bending load of 68kN for G1 and increased to 0.0114mm, at an axial and bending load of 335kN and 103kN, respectively, for G2.

- Along bolt holes at top and bottom locations, almost no stress concludes its sealing at the applied loading.

6 DETERMINATION OF JOINT LOAD CAPACITY USING SUPERPOSITION OF LOADS

For the combined loads application, a simple relationship derived by Abid [4] is used here to optimise the joint load capacity for the successful working of the joint as;

$$\frac{F}{F_{Max}} + \frac{P}{P_{Max}} + \frac{M}{M_{Max}} \leq 1 \qquad \text{---------- (3)}$$

Where;

F = *Actual axial load applied*

M = *Actual bending moment applied*

P = *Actual required fluid pressure applied*

F_{max} = *Maximum axial load permissible (calculated)*

M_{max} = *Maximum bending moment permissible*

P_{max} = *Maximum fluid pressure permissible*

Actual applied load during the experimental and FEA studies is substituted in above relationship and the joint capacity is determined in this study. Loads were applied in different magnitudes, i.e., less than and larger than the calculated values, in order to observe the joint behaviour. Stress results and observation have shown that the joints can take higher load than the calculated using code specified values. Results of joint strength and sealing capability for different cases are summarised in Table-2. Non-gasketed joint is observed to be safe up for strength and sealing up to an internal pressure plus axial loading of 180kN and at additional bending loading of 134 and 68kN for design and proof test pressures, respectively. The joint is found safe for sealing under combined design pressure, axial load (300kN) and bending load (100kN), and under combined

proof test pressure, axial load (335kN) and bending load (103kN). Results are summarized in Table-3.

7 CONCLUSIONS

From detailed experimental and FEA results, under combined internal pressure, axial and bending loading, almost static mode of load in the non-gasketed flange joint with positive taper angle profile is concluded. During this study a bolt up of 77% and 80% of the yield stress of the bolt material is applied for geometries G1 and G2, respectively, which resulted in slight variation in the bolt and flange stresses. However, a minimum bolt load of 80% of the yield stress for bolt material is concluded necessary for proper joint sealing for optimized performance. Flange geometry G1, is concluded better than the geometry G2 in terms of strength due to no observed yielding in flange, pipe and bolts. Flange geometry G2, is concluded better than the geometry G1 in terms of sealing, due to the proper contact from inside to outside diameter of flange face. Strength and sealing of the joint is concluded, under combined axial load of 180kN and bending load up to 134 and 68kN in addition to the design and proof test pressures, respectively. Application of bending loading in addition to applied axial and pressure load is concluded more critical for joint opening and possible leaks. Experimentally it is difficult to test different flange joint sizes; hence the methodology developed in this research is claimed as the base for the determination of each joint size under different loading conditions. Based on the conclusion of this study, for industrial applications, actual joint capacity for safe operating conditions can be determined.

8 ACKNOWLEDGEMENT

The authors are grateful to the Department of Mechanical Engineering, University of Strathclyde, Glasgow, UK for providing the test rig for the experimental work, and the Pakistan Science Foundation, Islamabad for providing funding to carry out this study.

9 RFERENCES

1. BS 1560. (1989). "Steel Pipe Flanges for the Petroleum Industry". *British Standards Institution,* London, UK.
2. "ASME Boiler and Pressure Vessel Code, Section VIII", (1998). *American Society of Mech. Eng.,* New York, USA.
3. Abid, M., Nash, D. H. (2004). "Comparative study of the behaviour of conventional gasketed and compact non-gasketed flanged pipe joints under bolt up and operating conditions". *International Journal of Pressure Vessels and Piping,* 80, 831-841.
4. Abid, M. (2000). Experimental and Analytical studies of conventional (gasketed) and unconventional (non gasketed) flanged pipe joints (with special emphasis on the engineering of 'joint strength' and 'sealing'). PhD Thesis.
5. Webjörn, J. (1967). "Flange Design in Sweden". *Petrochemical Mechanical Engineering Conference*, *American Society of Mechanical Engineers*, Philadelphia, USA. 17-20.
6. Webjörn, J. (1985). "The Bolted Joint - a Series of Problems". *Linköping Studies in Science and Technology*, Dissertation No. 130.
7. Abid, M., Nash, D. H., Webjörn, J. (2000). "The stamina of non-gasketed flanges". *Fatigue2000*, Cambridge, 575-584.
8. Abid, M., Nash, D. H., (2004). "A parametric study of metal-to-metal contact flanges with optimised geometry for safe stress and no-leak conditions". *International Journal of Pressure Vessels and Piping,* (81), 67-74.
9. Muhammad Abid, "Determination of safe operating conditions for non-gasketed flange joint under combined internal pressure and temperature" International Journal of Mechanics and Materials in Design by Springer. DOI 10.1007/s10999-005-4447-2. (2005) 2: 129-140.

10. Muhammad Abid, “Design and Analysis of Non-Gasketed Bolted Flanged Pipe Joint Under Combined Internal Pressure and Temperature Loading”, 3rd BSME-ASME International Conference on Thermal Engineering, Dhaka, Bangladesh. 20-22 December, 2006. pp1-9.
11. Bouzid, A.H., Derenne, Michel., Chaarani, Abbas., 1998. ‘Tightness Prediction of Bolted Flanged Connections Subjected to External Bending Moments’. ASME PVP Conference, pp 61-67.
12. Sawa, T., Shimizu, A., 2000. ‘A Stress Analysis of Pipe Flange Connections Subjected to External Bending Moment’. ASME PVP Conference, pp 85-94.
13. Sawa, T., Matsumoto, M., 2002. ‘FEM Stress Analysis and Sealing Performance in Pipe Flange Connections with Gaskets Subjected to Internal Pressure and External Bending Moment’. ASME PVP Conference, pp 81-89.
14. Sawa, T., Maezaki, W., Nagata, S., 2004. ‘Stress Analysis and Sealing Performance Evaluation of Pipe Flange Connections with Gaskets Subjected to Internal Pressure and External Bending Moment (Effect of Scatter in Bolt Preload)’. ASME PVP Conference, pp 137-143.
15. Sawa, T., Matsumoto, M., Ando, F., 2003. ‘FEM Stress Analysis and Sealing Performance in Pipe Flange Connections with Gaskets Subjected to External Bending Moment (Case where Internal Fluid is Liquid)’. ASME PVP Conference, pp 85-95.
16. Cao, J., Bell, A. J., “Elastic Analysis of a Circular Flange Joint Subjected to Axial Force”. International Journal of Pressure Vessels and Piping 55(1993), pp 435-449.
17. Koves, W. J., 2007. “Design for leakage in flange joints under external loads” International Journal of Pressure Vessels Technology. Transaction of ASME. (2007), Volume 129, Issue 2, pp. 334-337.
18. Abid, M. and Awan, A.W., 2007, “3-D Non-Linear Finite Element Analysis of Non-Gasketed Flange Joint under Combined Internal Pressure and Axial Loading”, ASME Pressure Vessels and Piping Conference, July 22-26, 2007, San Antonio, Texas, USA.

19. Abid, M., Awan, A.W., and Nash, D.H., 2008, "Stamina of a non-gasketed flange joint under combined internal pressure and axial loading", IMechE Journal of Process Mechanical Engineering, Vol. 222, Part E, pp. 143-155.
20. Abid, M., Awan, A.W., and Nash, D.H., 2010, "Performance of a non-gasketed flange joint under combined internal pressure and bending loading", ASCE Journal of Engineering Mechanics, 136, 1519, 2010.
21. "ASME Boiler and Pressure Vessel Code, Section II, Part D", (1998). *American Society of Mech. Eng.*, New York, USA.
22. BS 3692: 1967, "Specifications for ISO metric precision hexagonal bolts, screws and nuts".
23. Spence, J., Macfarlane, D. M. and Tooth, A. S. (1998). "Metal-to-Metal full face taper hub flanges: finite element model evaluation and preliminary plastic analysis". *Proc. Instn. Mech. Engrs*. 212 (E), 57-69.
24. ANSYS Inc., (2004) *ANSYS Elements Manual*, Seventh Edition.
25. PD 5500:1997, "Unfired Fusion Welded Pressure Vessels", British Standards Institution, London.

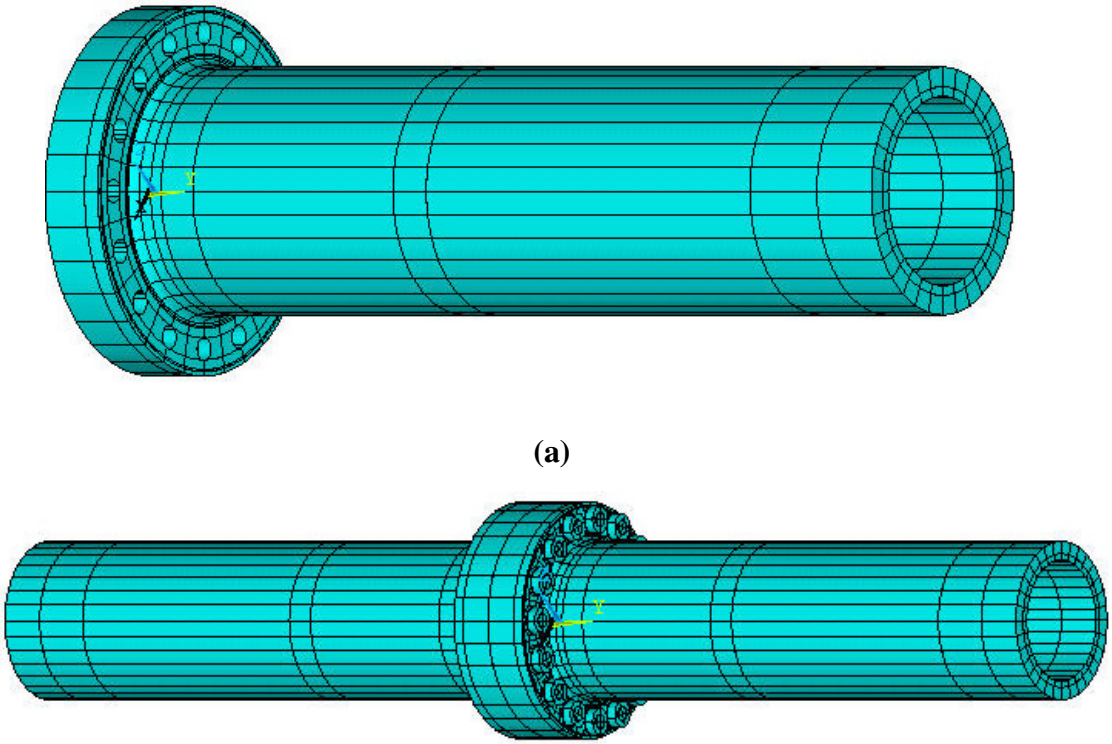

(a)

(b)

Figure 1: Complete 360 degree model of: (a) flange and pipe for one side, (b) joint assembly

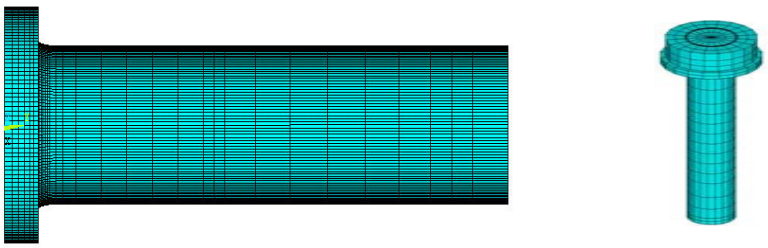

(a) **(b)**

Figure 2: Meshing of: (a) flange and pipe (b) bolt.

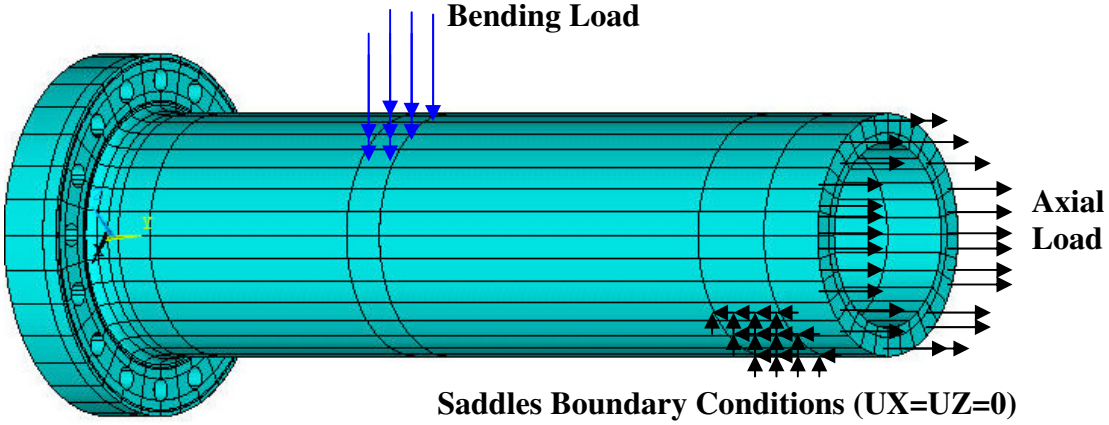

Figure 3: Internal pressure plus bending loading boundary conditions (right flange)

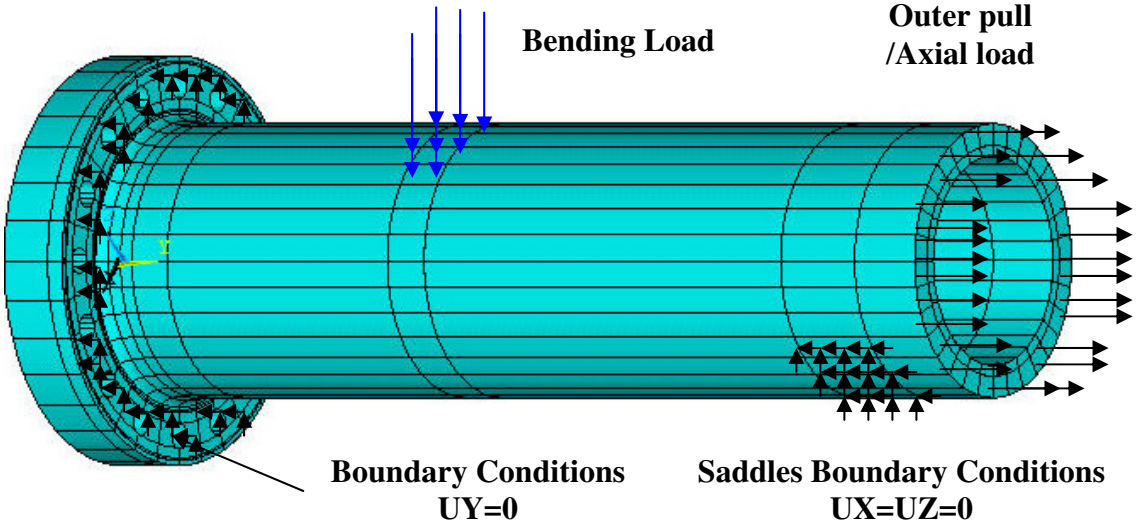

Figure 4: Internal pressure plus bending loading boundary conditions (left flange)

(a) **(b)** **(c)**

Figure 5: Non-gasketed flanges: (a) With O-ring groove, (b) Without O-ring groove (c) Tools used for joint assembly

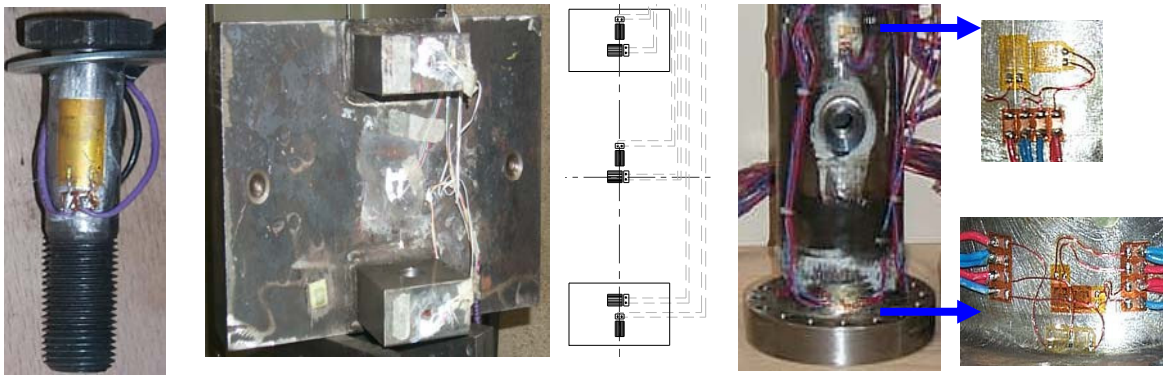

(a) **(b)**

Figure 6: Strain gauging of; (a) bolt (b) side frame (c) pipe and flange section

(a) (b)

Figure 7: Arrangement for (a) Internal pressure loading (b) combined loading

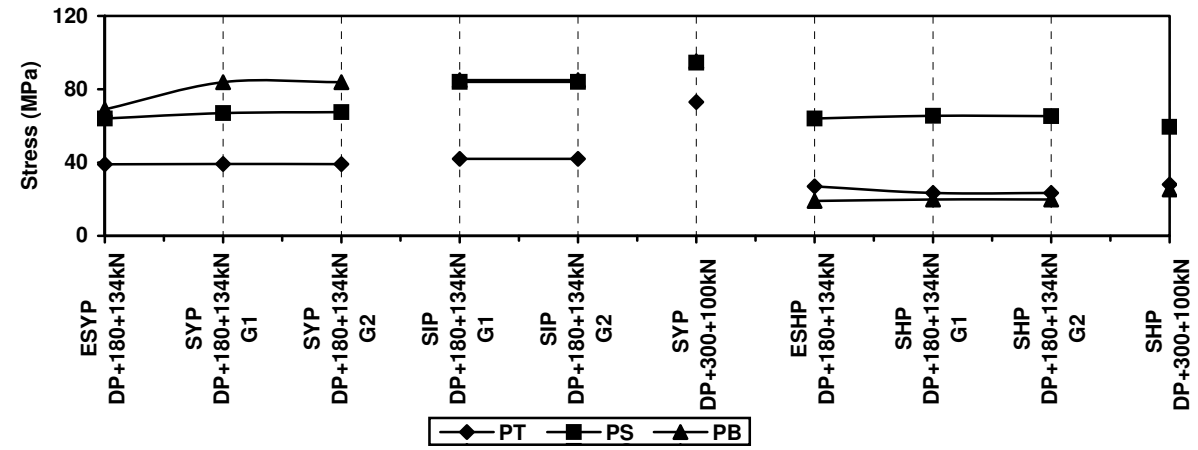

(a)

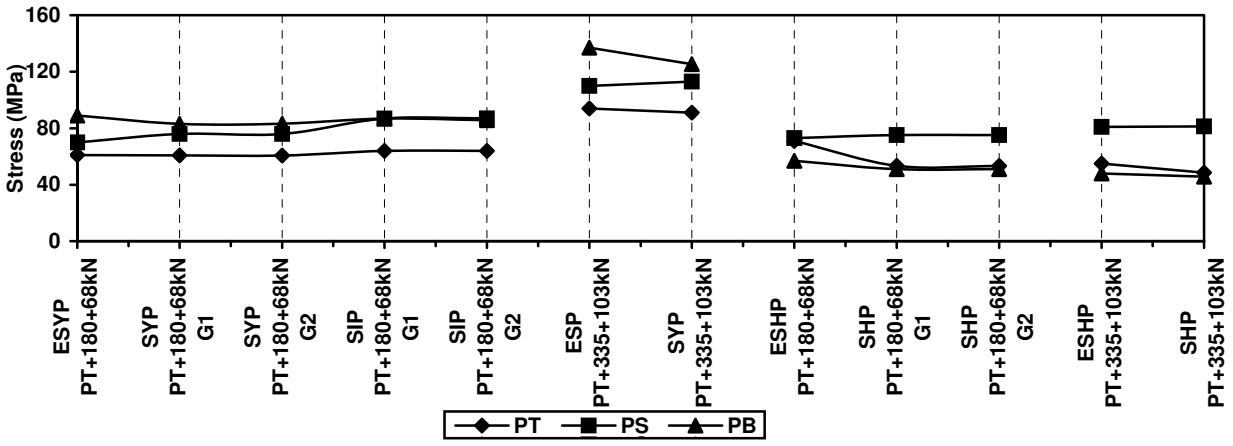

(b)

Figure 8: Stress variation at pipe (FEA vs. experimental results) (a) At Design pressure plus axial plus bending loading (b) At Proof test pressure plus axial plus bending loading

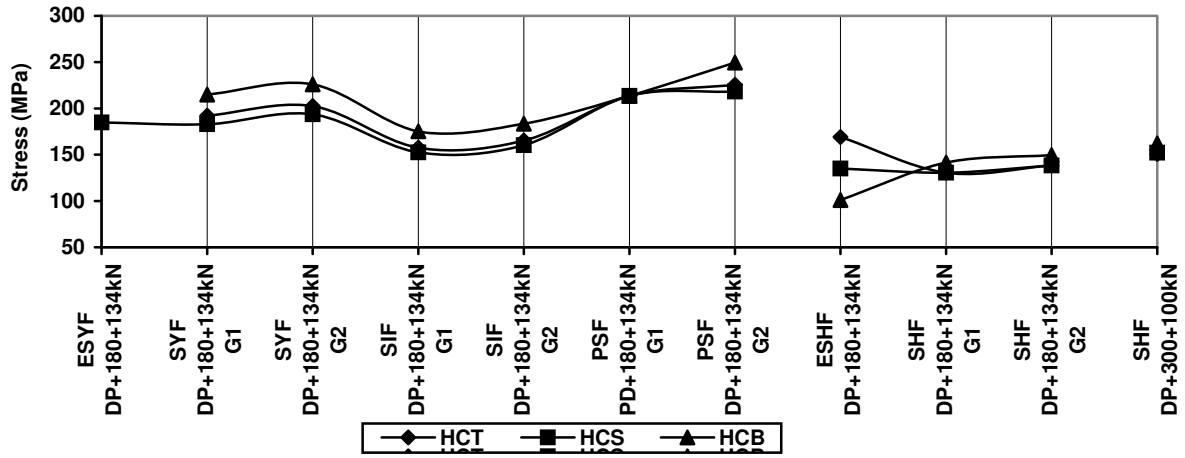

Figure 9: Stress variation at design pressure plus axial plus bending loading at hub centre (HCT= Hub Centre Top, HCS=Hub Centre Sides, HCB= Hub Centre Bottom)

(ESYF and ESHF are the experimental axial and hoop stresses while SIF, SYF, SHF and PSF are the stress intensity, axial, hoop and principle stresses at the flange hub centre)

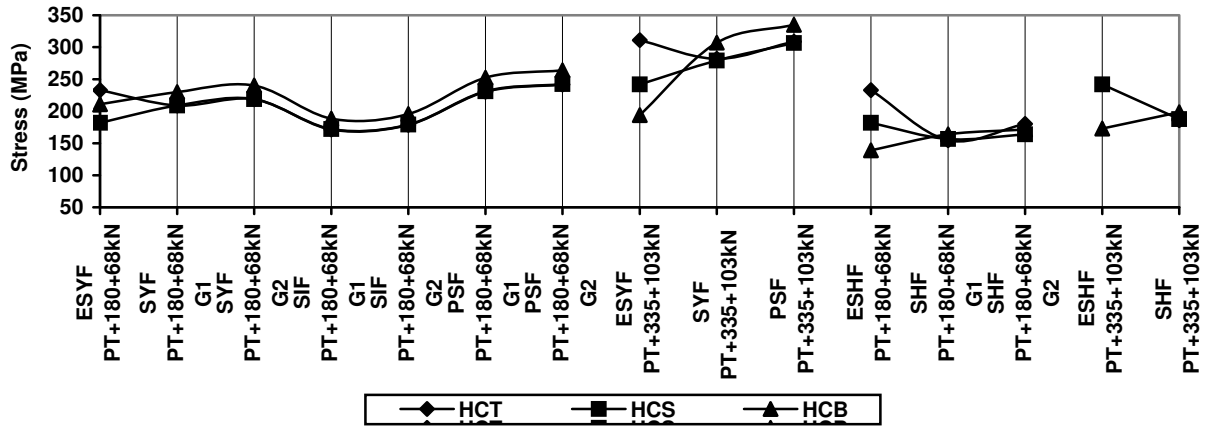

Figure 10: Stress variation at proof test pressure plus axial plus bending loading at hub centre (HCT= Hub Centre Top, HCS=Hub Centre Sides, HCB= Hub Centre Bottom) (ESYF and ESHF are the experimental axial and hoop stresses while SIF, SYF, SHF and PSF are the stress intensity, axial, hoop and principle stresses at the flange hub centre)

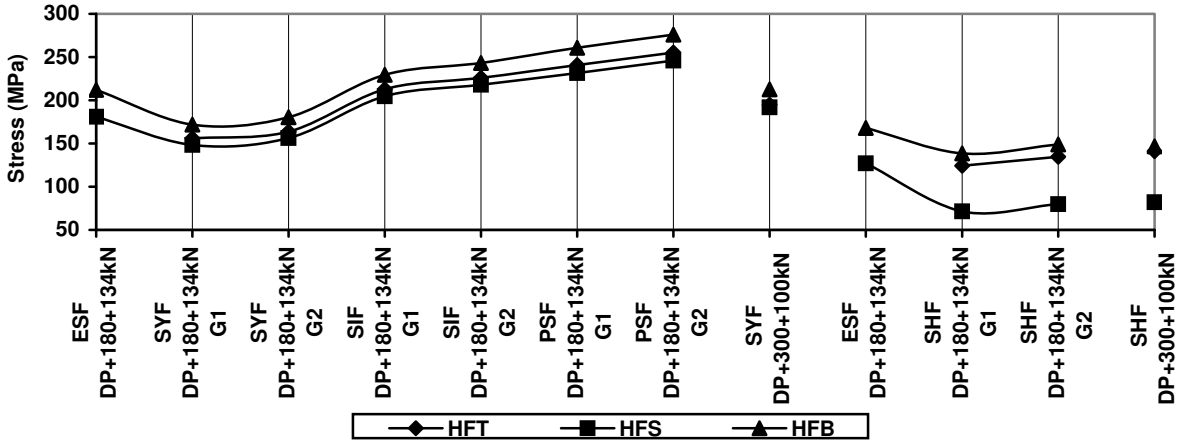

Figure 11: Stress variation at design pressure plus axial plus bending loading at hub flange fillet (HFT= Hub Flange Fillet Top, HFS= Hub Flange Fillet Sides, HFB= Hub Flange Fillet Bottom)

(ESYF and ESHF are the experimental axial and hoop stresses in MPa while SIF, SYF, SHF and PSF are the stress intensity, axial, hoop and principle stresses in MPa at the flange hub flange fillet)

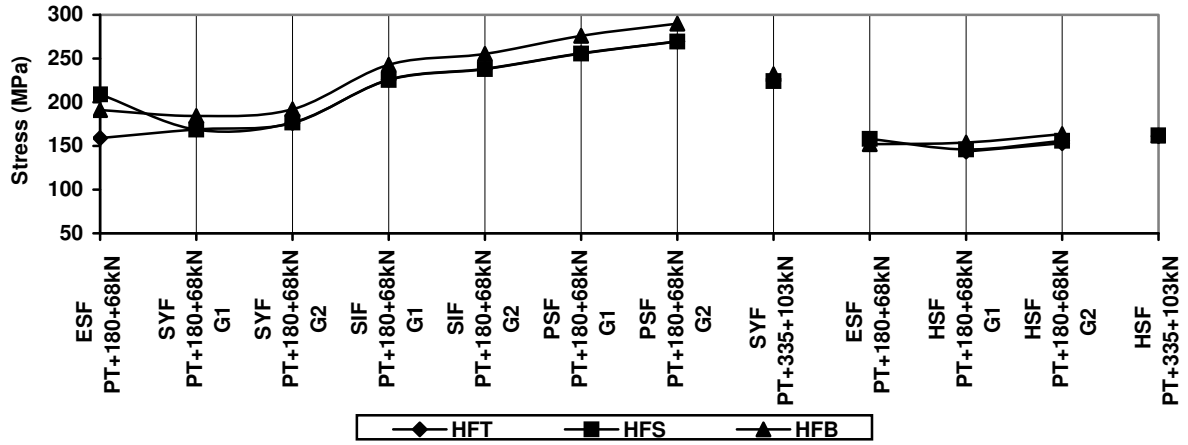

Figure 12: Stress variation at proof test pressure plus axial plus bending loading at hub flange fillet (HFT= Hub Flange Fillet Top, HFS= Hub Flange Fillet Sides, HFB= Hub Flange Fillet Bottom)

(ESYF and ESHF are the experimental axial and hoop stresses in MPa while SIF, SYF, SHF and PSF are the stress intensity, axial, hoop and principle stresses in MPa at the flange hub flange fillet)

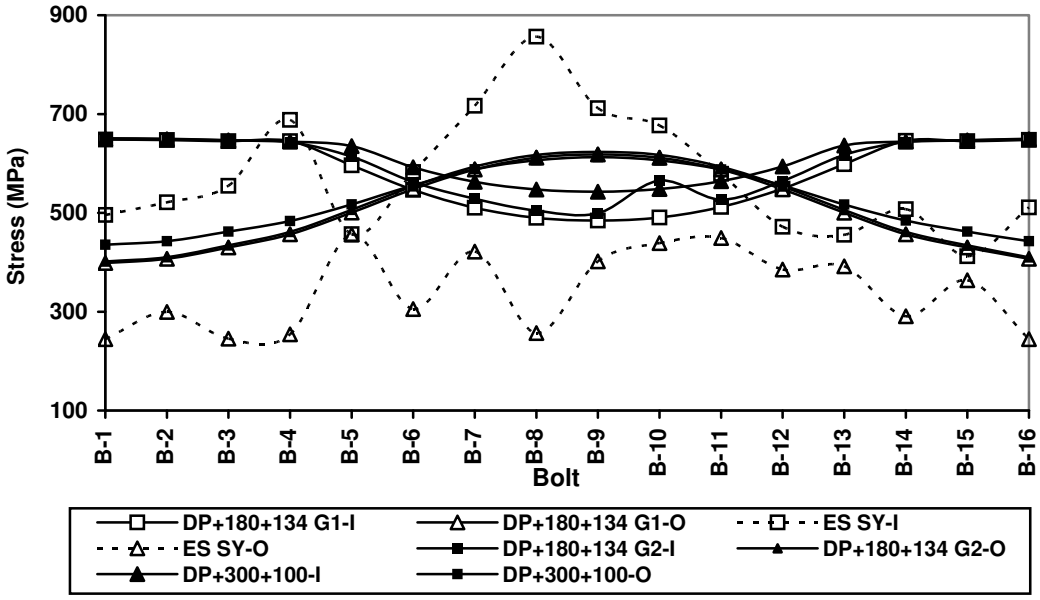

Figure 13: Stress variation in bolts at design pressure plus axial plus bending loading (ES SY-I and ES SY-O are the experimental axial stresses in MPa at the inside and outside node of the bolts)

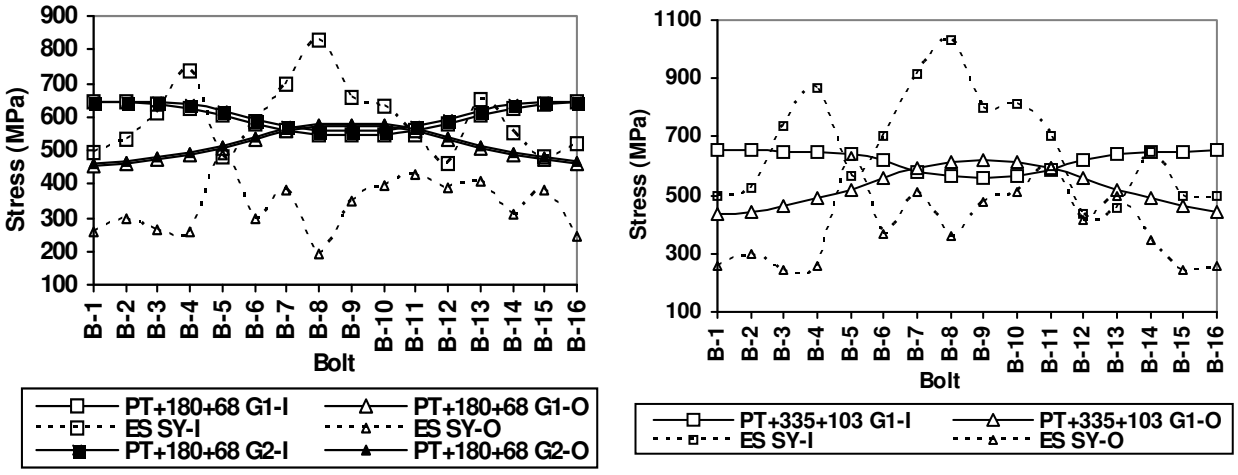

Figure 14: Stress variations in bolts at proof test pressure plus axial plus bending loading (ES SY-I and ES SY-O are the experimental axial stresses in MPa at inside and outside node of the bolts)

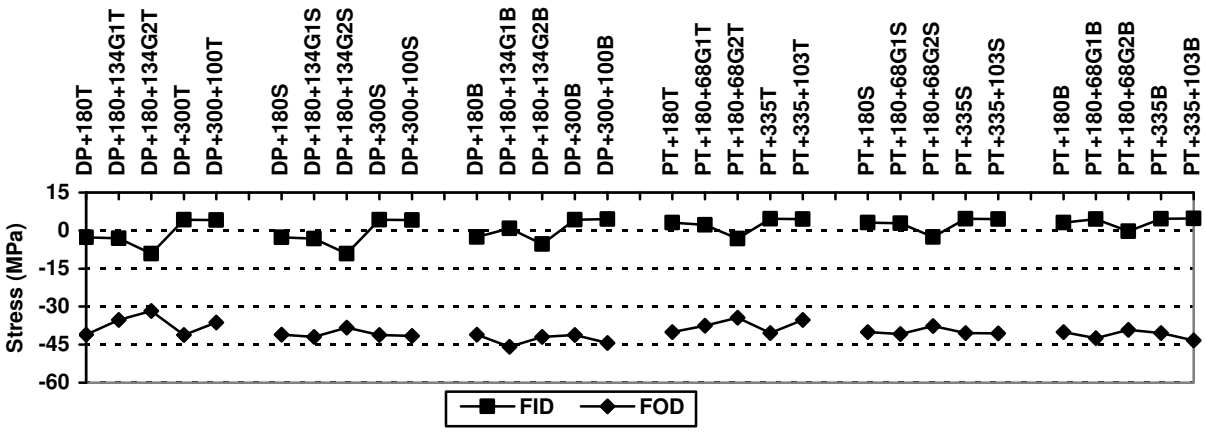

Figure 15: Contact stress variations at flange inside and outside diameters at design and proof test pressures plus axial plus bending loading (T=Top, B=Bottom, S=Side)

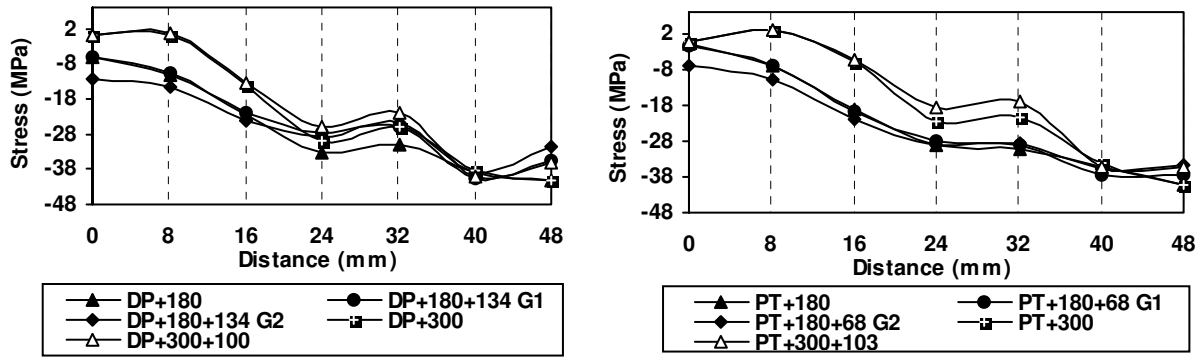

(a) **(b)**

Figure 16: Contact stress variations along bolt holes line at; (a) design pressure plus axial plus bending loading (b) proof test pressure plus axial plus bending loading

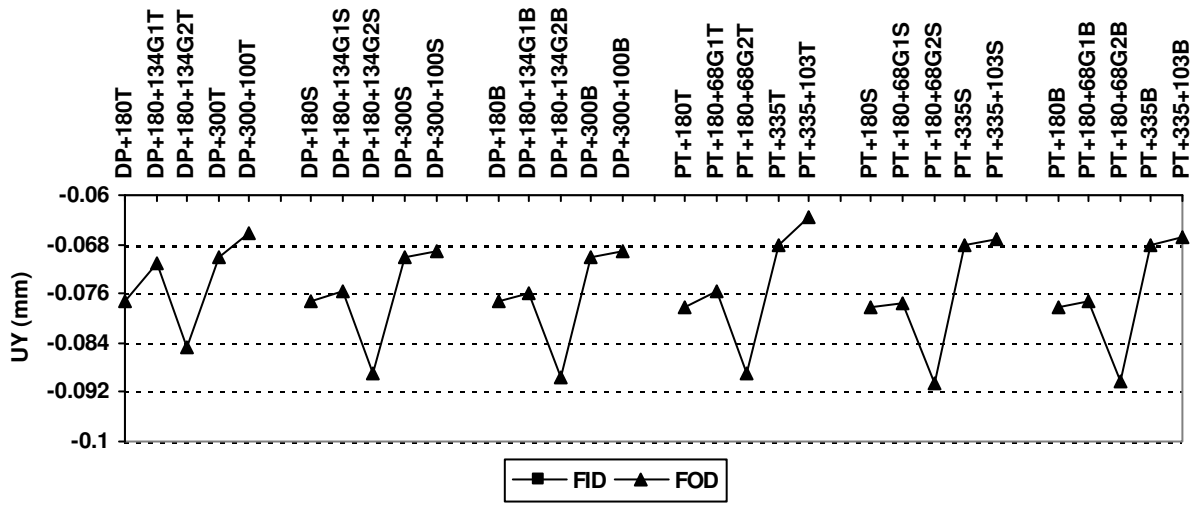

Figure 17: Axial flange displacements at design and proof test pressures plus axial plus bending loading at inside and outside diameters. (T=Top, B=Bottom, S=Side)

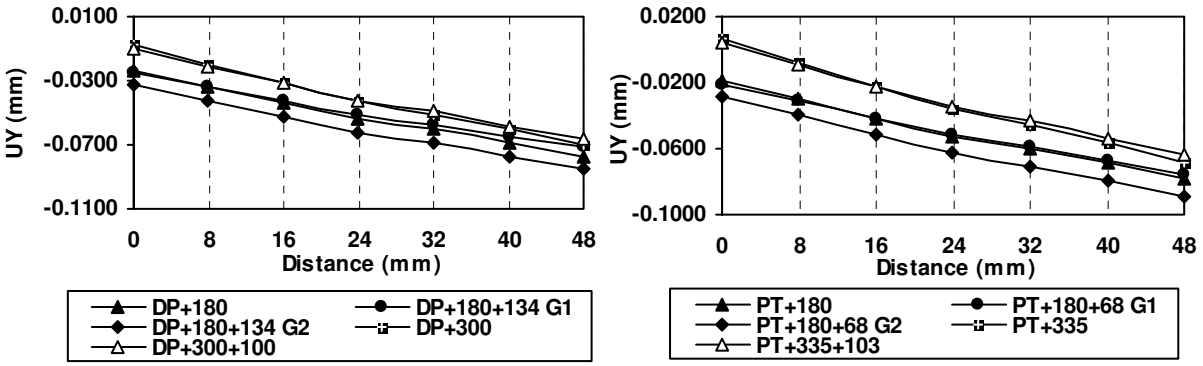

(a) **(b)**

Figure 18: Axial flange displacements along bolt hole lines at; (a) design pressure plus bending loading, (b) proof test pressure plus bending loading (100~188kN)

Table 1: Material Properties

Non-gasketed joint components	E (MPa)	υ	Allowable Stress (MPa)
Flange/ Pipe [18]	203395	0.3	248.2
Bolt and Washer [19]	204000	0.3	640

Table-2: **Load carrying capacities of non-gasketed flange joint**

F	P	M	F_{max}	P_{max}	M_{max}	F/F_{max}	P/P_{max}	M/M_{max}	$F/F_{max} + P/P_{max} + M/M_{max}$	Extra Load applied
kN	MPa	kNm	kN	MPa	kNm					(%)
173	15.3	20.28	388	23.0	12.44	0.45	0.67	1.63	2.74	174.13
180	15.3	17.42	388	23.0	12.44	0.46	0.67	1.40	2.53	152.95
173	23.0	11.7	342	23.0	12.09	0.51	1.00	0.97	2.47	147.37
180	23.0	8.84	342	23.0	12.09	0.53	1.00	0.73	2.26	125.76

Table-3: Strength and sealing capability determined from FE Analysis

S. No	Loading Type	Loading Range
		STRENGTH
1	DP+AL+BL	Should be less than DP+180+134kN
2	PT+AL+BL	Should be less than PT+180+68kN
		SEALING
1	DP+AL+BL	No Leak up to DP+300+100kN
2	PT+AL+BL	No Leak up to PT+335+103kN